PSFC/JA-00-23

High Resolution Edge Thomson Scattering Measurements on the Alcator C-Mod Tokamak

J. W. Hughes, D. A. Mossessian, A. E. Hubbard,
E. S. Marmar, D. Johnson[†], D. Simon[†]

August 2000

Plasma Science and Fusion Center
Massachusetts Institute of Technology
Cambridge, Massachusetts 02139

[†]Plasma Physics Laboratory
Princeton University
Princeton, New Jersey 08544

Submitted to *Review of Scientific Instruments*. (Presented as a poster at the 13th Topical Conference on High Temperature Plasma Diagnostics, Tucson, Arizona, June 18–22, 2000.)

This work was supported in part by the U.S. Department of Energy Contract No. DE-FC02-99ER54512.

Abstract
A high resolution Thomson scattering diagnostic is in operation on the Alcator C-Mod tokamak, measuring radial profiles of electron temperature and density at the plasma edge. Photons are scattered from an Nd-YAG laser beam pulsed at 30 Hz (1.3-J, 8-ns pulse), and are measured by a filter polychromator with four spectral channels. The polychromator measures T_e in the range of 15–800 eV and n_e of 0.3–3$\times 10^{20}$ m^{-3}. Twenty scattering volumes are located about the last closed flux surface, spaced for a nominal resolution of 1.3 mm in midplane radial coordinates. High resolution is essential for measuring edge T_e and n_e profiles on C-Mod, since these quantities exhibit gradient scale lengths as small as 2 mm in *H*-mode. The steep profiles at the *H*-mode edge are fit to a parameterized pedestal function for ease of analysis. Measured profiles are compared with edge profiles from electron cyclotron emission and visible continuum diagnostics.

I. INTRODUCTION

In tokamak fusion experiments, the formation of a transport barrier at the plasma edge is observed upon transition from the low confinement mode (*L*-mode) to the high confinement mode (*H*-mode).[1] The barrier is characterized by a pronounced steepening in the radial profiles of both electron density (n_e) and electron temperature (T_e). This region is commonly called the pedestal region, due to the typical shape of the edge profiles. Because factors like core plasma confinement and edge stability are known to be sensitive to conditions in the pedestal region, accurate and well-resolved pedestal measurements are desirable.

The Alcator C-Mod tokamak[2] ($R = 0.67$ m, $a = 0.22$ m) has an *H*-mode pedestal region less than 1 cm in width. Within this or a lesser distance, plasma n_e can fall from more than 10^{20} m^{-3} to below 10^{19} m^{-3}. Likewise, T_e can drop from several hundred eV to less than 10 eV. Measurements of these parameters in the pedestal region must therefore be made with high spatial resolution. A Thomson scattering (TS) diagnostic with 1.3 mm nominal radial resolution has been implemented on Alcator C-Mod, in order to characterize the T_e and n_e pedestals in *H*-mode.

II. INSTRUMENT DESCRIPTION

The edge TS diagnostic uses a Continuum PowerLight 9030 Nd:YAG laser with 1.5 J pulse energy, 10 ns pulse duration, and a repetition rate of 30 Hz. The beam is steered through a vertical port of the tokamak and maintained at a major radius of 0.69 m. Scattered light is focused onto collection fiber optics by an $f/7$ Cooke triplet with a demagnification of 1:2.[3] Twenty collection fibers

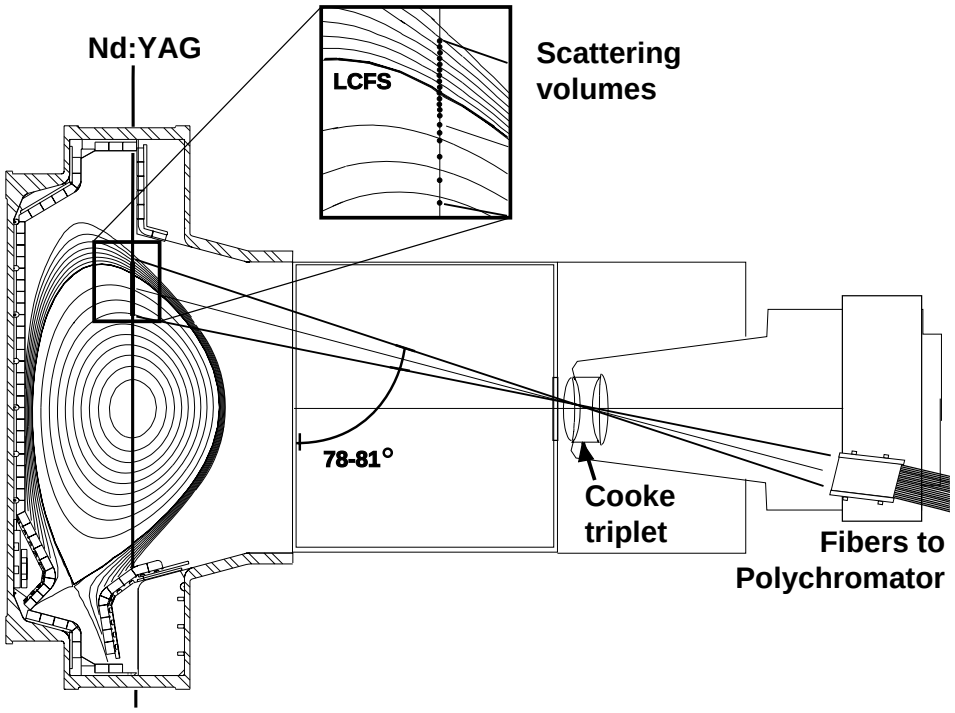

Figure 1: Alcator C-Mod cross-section and layout of TS collection optics. The Cooke triplet is $f/7$ with a demagnification of 1:2. 1-mm diameter collection fibers are mounted in the image plane. Scattering locations are clustered about the LCFS at the upper plasma edge.

measuring 1.2 mm in diameter are positioned so that they image scattering volumes at the upper edge of the plasma, as shown in Fig. 1. Ray tracing calculations indicate an imaged spot size of 1 mm for scattering locations 30 cm above the optical axis. Misalignment of the beam with respect to the collection fibers can be corrected by changing voltages on three independent piezoelectric mounts, which adjust the beam steering mirrors. To evaluate misalignment, two alignment fibers are arranged on either side of the fiber with the innermost plasma view. With optimal alignment, over 95% of the observed signal falls in the central channel. Beam misalignment is detected as excess signal in either alignment fiber.

The fibers transmit light to an imaging filter polychromator,[4] which has 25 spatial channels in four spectral bands. The layout of the polychromator is presented in Fig. 2. The polychromator input lens focuses light from the

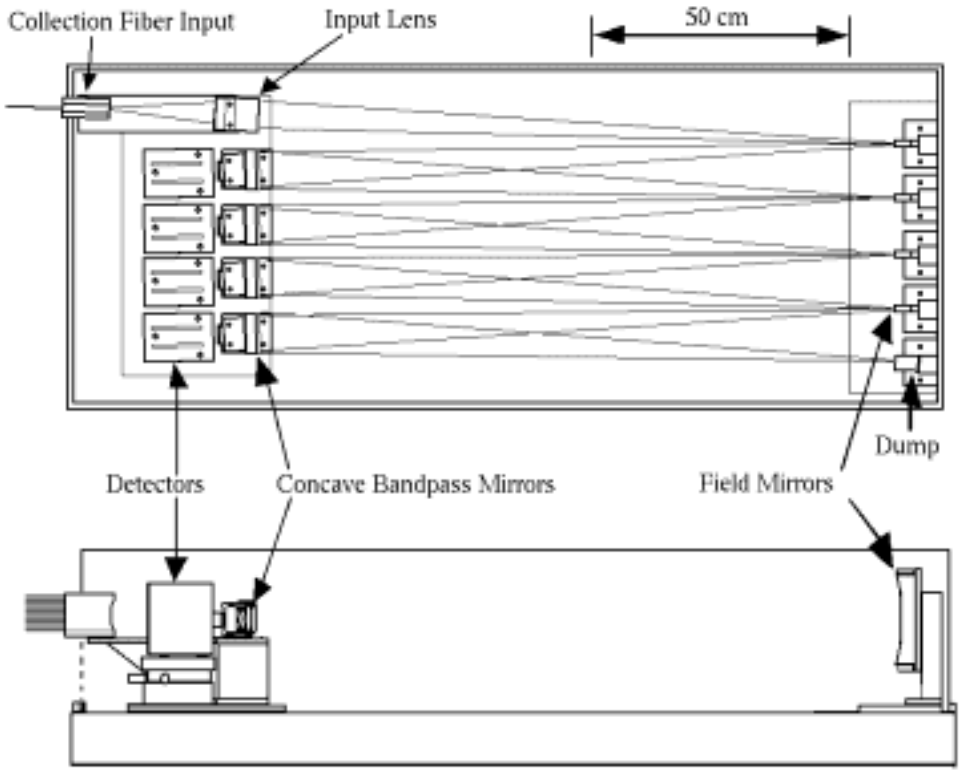

Figure 2: Layout of four-channel polychromator; plan and side views. The detectors measure TS in four bandpasses, with good rejection of the laser line.

collection fibers onto the first of a series of four concave mirrors. Each of these mirrors acts as a field element, imaging the fiber spots onto a successive circular concave mirror. Each circular mirror has a multilayer dielectric filter coating that transmits light in a particular bandpass. The light that is reflected from each of these bandpass filters is focused onto the next field mirror in the series, or, in the case of the fourth filter, onto a dump. The filters are designed to have very high rejection of the laser line ($\lambda = 1064$ nm), and the field mirrors are coated with a narrow pass dielectric filter that transmits the laser line. The result is a high degree of stray light attenuation. A blocking filter is placed on the polychromator input lens in order to reject background light outside the range of the four bandpasses.

Light transmitted through each bandpass filter is focused onto a 25-element avalanche photodiode (APD) array. Each array element is 300×250 μm, and there is 50 μm of dead space between elements. The focus and alignment

of the image spots on the APDs is optimized by backlighting the collection fibers and adjusting the APD positions until the cross-talk between adjacent APDs is minimized. Because the focus and alignment are sensitive to small changes in position, thermal expansions and contractions within the position control mechanism must be minimized. In addition, APD response is highly sensitive to temperature. Thus, the polychromator is enclosed in thermal insulation, while automatically regulated heaters maintain a constant internal temperature of 32°C.

The APD signals have a both pulse contributions from TS and slowly varying contributions from plasma background light. The plasma background signal is isolated and subtracted from the total signal by the detector circuitry, which is described in Ref. 4. Because both the slow and pulse signals contribute to the noise in the TS measurements, both signals are sampled and digitized. A fraction of the Nd:YAG beam leaking through a steering mirror atop the tokamak is used to trigger the sampling hardware. The diagnostic is controlled using standard CAMAC hardware driven by MDS-Plus data acquisition software.[5]

III. CALIBRATION AND DATA ANALYSIS

To fit T_e and n_e to the measured signals, we use the Thomson spectral form factor, $S(T_e, \theta_i, \lambda)$, with relativistic corrections, as given by Sheffield.[6] Here, θ_i is the scattering angle of the i-th spatial point. The expected response to Thomson scattered light in the j-th spectral channel for the i-th spatial point is then given by

$$I_{i,j}(n_e, T_e) = n_e E_0 \left(\frac{d\sigma}{d\Omega}\right)^{\mathrm{TS}} A_i C_{i,j} \int_0^\infty f_j(\lambda) S(T_e, \theta_i, \lambda)\, d\lambda \ , \qquad (1)$$

where E_0 is the laser energy, $\left(\frac{d\sigma}{d\Omega}\right)^{\mathrm{TS}}$ is the differential cross section for TS, and the $f_j(\lambda)$ are the normalized instrument functions of the spectral channels. The calibration factors, $C_{i,j}$, give the relative response of all the spectral channels, while the A_i are absolute sensitivity coefficients for the spatial channels. Data analysis routines fit experimentally measured signals to Eq. 1 with T_e and n_e as fitting parameters. We thus require a series of calibrations to obtain $f_j(\lambda)$, $C_{i,j}$, and A_i.

To measure the $f_j(\lambda)$, we focus onto the APD arrays the output of a scannable monochromator with known spectral intensity. The spectral response of each APD array is measured and normalized to the monochromator output. Fig. 3 shows the normalized instrument functions, along with $S(T_e, \lambda)$ at $\theta_i = 90°$, for two values of T_e. The integral DC response of the individual channels is measured by illuminating the collection fibers with a source of

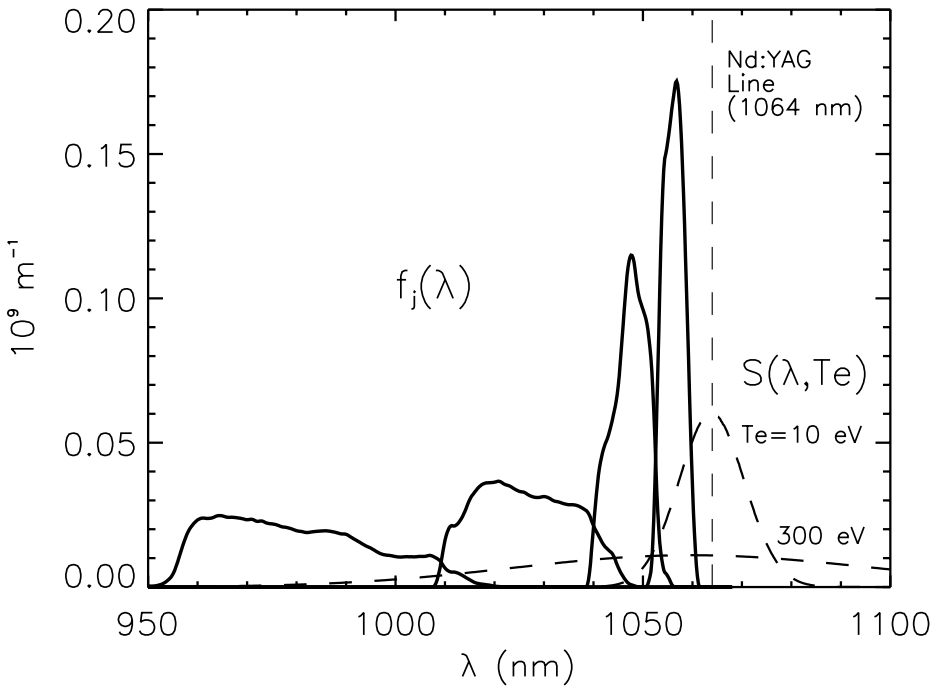

Figure 3: Edge TS polychromator instrument functions, f_j. Spectral distributions of Thomson light at 10 and 300 eV ($\theta = 90°$) are also shown.

known spectral brightness. The APD response to a fast pulse source in general differs from the DC response, and so the relative responses to quickly varying ($\sim$ 10 ns) and to slowly varying ($> 1\mu$s) signals are measured independently. This is done by directly illuminating the APD arrays with the output of a laser diode, which is operated first in short pulse mode, and second in long pulse mode. The results of the DC and pulsed calibrations are combined, yielding the $C_{i,j}$ in Eq. 1.

Knowing $S(T_e, \theta_i, \lambda)$, $f_j(\lambda)$, and $C_{i,j}$ enables us to measure T_e at the i-th spatial location. In order to calculate n_e from experimental TS signals, we obtain absolute sensitivity coefficients, A_i, using Raman scattering (RS) in D_2.[7] Rotational anti-Stokes lines of known wavelength, $\lambda_k^{\rm RS}$, are measured in the polychromator spectral channels. The A_i are computed from the RS signal, $I_{i,j}^{\rm RS}$; the laser energy, E_0; the molecular density of the scattering gas, $n_{\rm D_2}$; the differential cross sections for scattering into the k-th rotational line, $\left(\frac{d\sigma}{d\Omega}\right)_k^{\rm RS}$;

and the calibration terms $C_{i,j}$, $f_j(\lambda_k^{\rm RS})$. Several fill pressures in the range of 0–500 torr are used, and at least 1000 RS measurements are made at each pressure, in order to minimize statistical uncertainty. Due to high rejection of the laser line, neither stray light nor Rayleigh scattering is measured.

Based on the above calibrations, look-up tables of polychromator signals are constructed as functions of T_e. Experimental signals are fit to these tables using a non-linear least squares fitting routine, and both T_e and n_e are obtained. By measuring the signals in the alignment channels and comparing with that in the central channel, we can evaluate whether laser misalignment occurs, and correct n_e measurements that would otherwise be underestimated. The scattering locations are mapped to the tokamak midplane along surfaces of constant magnetic flux using results from the EFIT magnetics reconstruction code.[8] Assuming that T_e and n_e remain constant along flux surfaces, this mapping gives midplane radial profiles of these quantities. The finite collection fiber diameter results in a minimum radial resolution of 1.3 mm. The Nd:YAG repetition rate gives a temporal resolution of 33.3 ms.

When edge profiles form pedestals, they are fit to a parameterized function, f, on $R' = R - R_{0f}$, where R is midplane radius and R_{0f} is the position of the pedestal center:

$$f(R') = b_f + \frac{h_f}{2}\left[\tanh\left(\frac{R'}{\delta_f}\right) + 1\right] - m_f(R' + \delta_f)H[-(R' + \delta_f)] \qquad (2)$$

Here, b_f is the pedestal baseline and h_f is its height. The width is given by, $\Delta_f = 2\delta_f$. The Heaviside function, $H[-(R'+\delta_f)]$, allows one to account for the finite radial slope, $-m_f$, that exists inside the pedestal region. Pedestals are characterized using the parameters, h_f, Δ_f, and R_{0f}, and also the maximum radial gradient, which is obtained according to $|\nabla f|_{\rm max} = h_f/\Delta_f$, and is located at $R = R_{0f}$.

IV. SUMMARY OF EXPERIMENTAL RESULTS

We measure T_e from 15 to 800 eV at n_e in the range of 0.3–2.5$\times 10^{20}$ m^{-3}. The dynamic range in both T_e and n_e allows complete coverage of Alcator C-Mod edge profiles in *H*-mode, with uncertainties that are typically 5–20%. Profiles of T_e and n_e measured at time points before and after the *H*-mode transition are shown in Fig. 4 to illustrate the steepening in parameter gradients that characterizes high confinement.

Once a plasma is in *H*-mode, parameter profiles generally are well fit with the pedestal function of Eq. 2. When the *H*-mode is fully developed, the density pedestal height, h_n, is roughly 0.7 times the central plasma n_e, and the width, Δ_n, typically ranges from 2 to 8 mm. The temperature pedestal

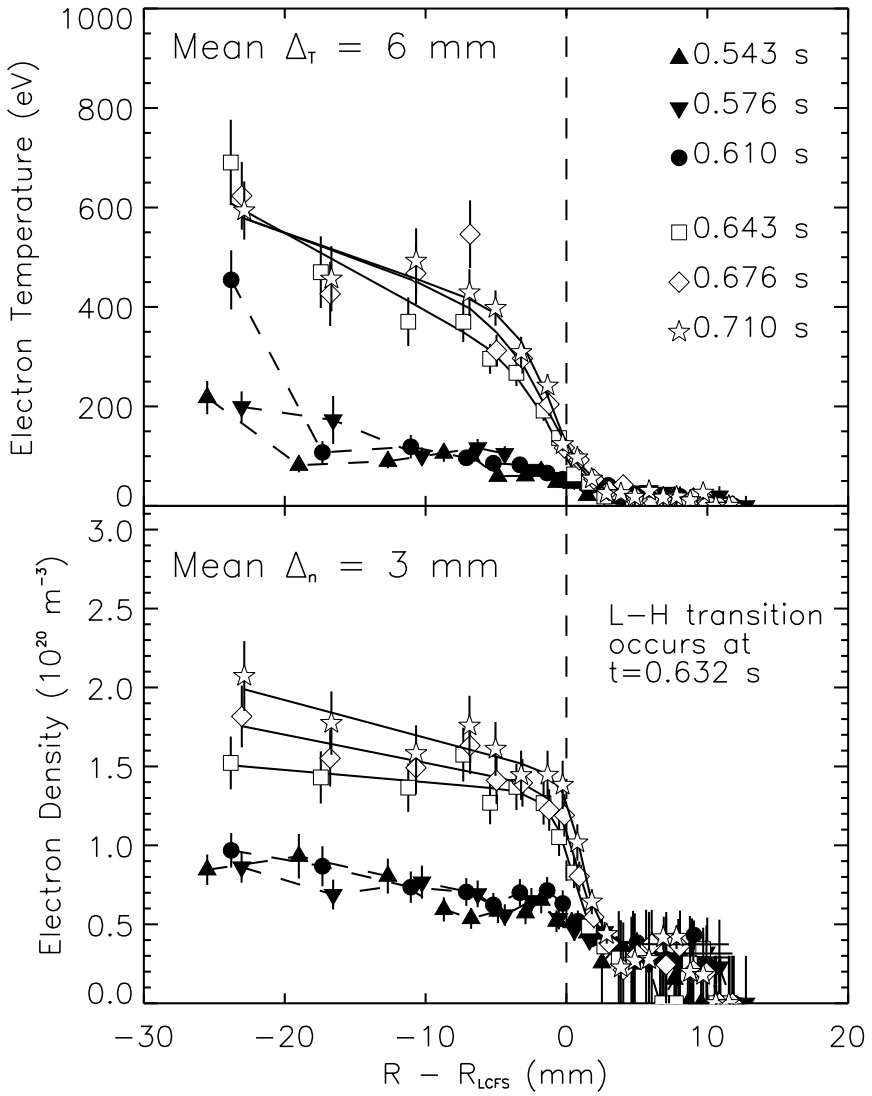

Figure 4: Edge profiles of T_e and n_e before and after *L-H* transition. Error bars on T_e and n_e reflect estimated statistical uncertainties; also, n_e error bars account for uncertainties in the absolute calibration.

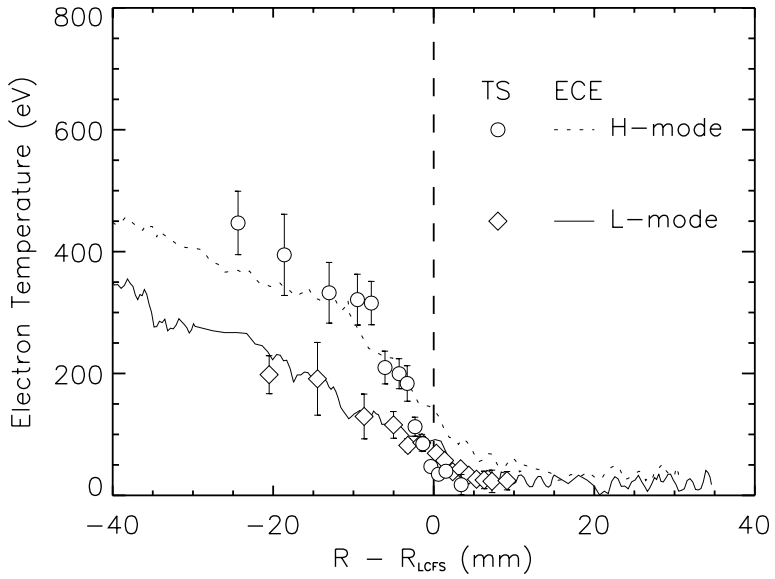

Figure 5: Comparison of TS and ECE T_e profiles in *L*- and *H*-mode. Each ECE profile was recorded during a 150-ms sweep of B_Φ. The plotted TS profiles are averages over the duration of the sweep.

exhibits a similar range of widths, but the height, h_T, depends on the plasma heating mechanism and confinement characteristics. Temperature pedestal heights from 150 to 400 eV have been observed. Both the n_e and T_e pedestals are located inside the LCFS. The T_e pedestal is typically 1 mm inside the n_e pedestal.

Edge T_e profiles can also be obtained using electron cyclotron emission (ECE), as measured by a nine-channel grating polychromator. This diagnostic gives midplane T_e at nine radial locations, corresponding to nine distinct magnetic field values. By sweeping the toroidal field by 2–3% over a period of 100–200 ms, we obtain a radial scan of the T_e pedestal,[9] the radial resolution of which is instrument-limited to 9 mm. In steady-state plasmas the TS temperatures during the sweep are time averaged and compared with the ECE profile. Due to uncertainties in both the location of these measurements and the EFIT mapping of TS points to the midplane, the profiles exhibit a variable relative shift, usually 5–10 mm, that must be corrected. This shift has been removed in Fig. 5, which compares profiles obtained in *L*-mode and *H*-mode plasmas. Agreement between ECE and TS is generally very good in *L*-mode. In *H*-mode TS measurements give h_T 10–20% larger than that

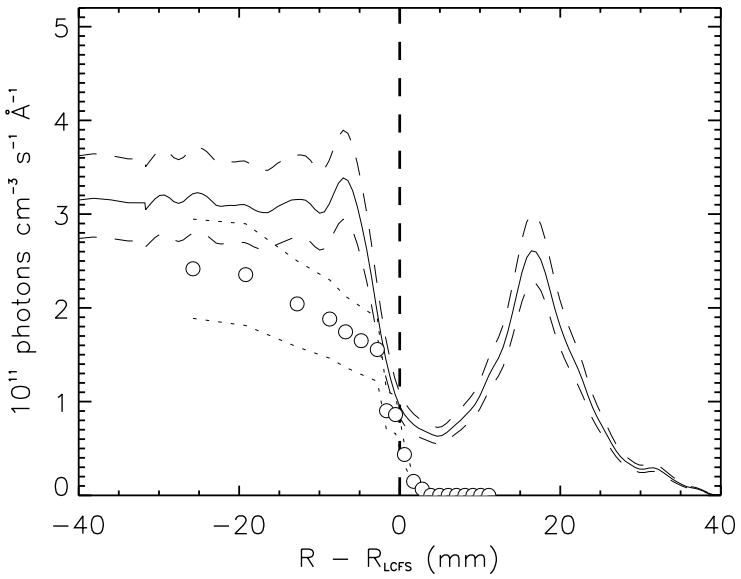

Figure 6: TS profiles are compared to visible emissivity measurements (solid curve) by calculating bremsstrahlung emissivity profiles (circles) from T_e and n_e. The error envelopes given by the dashed and dotted lines reflect uncertainties in absolute calibration of either instrument.

from ECE, probably due to uncertainties in the $f_j(\lambda)$ and $C_{i,j}$ described in Section II. The pedestal width measured with TS is routinely smaller than the 9-mm resolution of ECE.

Comparison also is made with measurements from a high-resolution visible continuum array, which measures line-integrated plasma emissivity at 536 nm along tangential chords. An Abel-inversion produces radial emissivity profiles with 1 mm resolution. To compare these profiles with TS results, free-free bremsstrahlung emissivity is calculated from the Thomson T_e and n_e profiles, and the estimated value of $Z_{\rm eff}$, usually between 1 and 2, at the plasma center. These profiles are compared in *H*-mode plasmas as in Fig. 6, again after relative shifts are introduced. The measured emissivity profile contains a significant component on and outside the LCFS that is not due to bremsstrahlung, and is thought to show a contribution from molecular deuterium. In addition, a bump occurring consistently at the top of the emissivity pedestal is thought to be an artifact of the inversion process. Ignoring these features, reasonable agreement exists between the measured and calculated emissivity pedestals. The widths in general agree, while the amplitude of the measurement is consistently higher

than the height of the calculated pedestal. This discrepancy is consistent with the expected uncertainties of 10–15% in the absolute calibrations of both instruments, as well as the uncertainty in $Z_{\rm eff}$.

V. CONCLUSION

The edge TS diagnostic on Alcator C-Mod provides information on plasma conditions near the LCFS. In this region the electron temperature and density profiles have been measured with 1.3-mm radial resolution, and with 33.3-ms temporal resolution. Edge T_e and n_e profiles are obtained over a dynamic range of 15–800 eV and 0.3–3.0$\times 10^{20}$ m^{-3}, respectively, allowing complete characterization of *H*-mode pedestals, which can be as narrow as 2 mm. Systematic errors of 10–20% may exist in the T_e and n_e measurements and are the subject of ongoing evaluation. Within the bounds of measurement uncertainty, comparisons with midplane ECE and visible continuum diagnostics show reasonable agreement.

VI. ACKNOWLEDGEMENTS

We would like to acknowledge the contributions to the edge Thomson scattering hardware provided by Princeton Scientific Instruments. This work is supported by DOE Coop. Agreement DE-FC02-99ER54512.

References

1. ASDEX Team, Nucl. Fusion **29**, 1959 (1989).

2. I. H. Hutchinson, R. Boivin, F. Bombarda, P. Bonoli, S. Fairfax, C. Fiore, J. Goetz, S. Golovato, R. Granetz, M. Greenwald, S. Horne, A. Hubbard, J. Irby, B. LaBombard, B. Lipschultz, E. Marmar, G. McCracken, M. Porkolab, J. Rice, J. Snipes, Y. Takase, J. Terry, S. Wolfe, C. Christensen, D. Garnier, M. Graf, T. Hsu, T. Luke, M. May, A. Niemczewski, G. Tinios, J. Schachter, and J. Urbahn, Phys. Plasmas **1**, 1511 (1994).

3. R. Watterson and K. Chen, Rev. Sci. Instrum. **61**, 2867 (1990).

4. D. Dimock, B. Grek, D. Johnson, B. LaBombard, B. Lipschultz, and G. McCracken, Rev. Sci. Instrum. **68**, 700 (1997).

5. J. A. Stillerman, T. W. Fredian, K. A. Klare, and G. Manduchi, Rev. Sci. Instrum. **68**, 939 (1997).

6. J. Sheffield, *Plasma Scattering of Electromagnetic Radiation*, Academic, New York (1975).

7. H. Röhr, Phys. Lett. **81A**, 451 (1981).

8. L. L. Lao, H. St. John, R. D. Stambaugh, A. G. Kellman, and W. Pfeiffer, Nucl. Fusion **25**, 1611 (1985).

9. A. E. Hubbard, R. L. Boivin, R. S. Granetz, M. Greenwald, I. H. Hutchinson, J. H. Irby, Y. In, J. Kesner, B. LaBombard, Y. Lin, J. E. Rice, T. Sunn Pedersen, J. A. Snipes, P. C. Stek, Y. Takase, S. M. Wolfe, and S. Wukitch, Phys. Plasmas **5**, 1744 (1998).

10. E. S. Marmar, *et al.*, these Proceedings.